

Research Article

Different carbon sources affect lifespan and protein redox state during *Saccharomyces cerevisiae* chronological ageing

F. Magherini^{a,*}, A. Carpentieri^b, A. Amoresano^b, T. Gamberi^a, C. De Filippo^c, L. Rizzetto^{c,d}, M. Biagini^a, P. Pucci^b and A. Modesti^a

^a Dipartimento di Scienze Biochimiche Università degli Studi di Firenze, Viale G. Morgagni 50 I-50134, Firenze (Italy), Fax: +39 055 459 8905, e-mail: francesca.magherini@unifi.it

^b Dipartimento di Chimica Organica e Biochimica, Università di Napoli Federico II (Italy)

^c Dipartimento di Farmacologia Preclinica e Clinica, Università degli studi di Firenze (Italy)

^d Dipartimento di Genetica, Antropologia, ed Evoluzione, Università di Parma, Parma (Italy)

Received 15 September 2008; received after revision 17 December 2008; accepted 06 January 2009

Online First 6 February 2009

Abstract. In this study, a proteomic approach that combines selective labelling of proteins containing reduced cysteine residues with two-dimensional electrophoresis/mass spectrometry was used to evaluate the redox state of protein cysteines during chronological ageing in *Saccharomyces cerevisiae*. The procedure was developed on the grounds that biotin-conjugated iodoacetamide (BIAM) specifically reacts with reduced cysteine residues. BIAM-labelled proteins can then be selectively isolated by streptavidin

affinity capture. We compared cells grown on 2% glucose in the exponential phase and during chronological ageing and we found that many proteins undergo cysteine oxidation. The target proteins include enzymes involved in glucose metabolism. Both caloric restriction and growth on glycerol resulted in a decrease in the oxidative modification. Furthermore, in these conditions a reduced production of ROS and a more negative glutathione half cell redox potential were observed.

Keywords. Yeast, two-dimensional electrophoresis, chronological ageing, caloric restriction, proteins oxidation.

Introduction

The yeast *Saccharomyces cerevisiae* is a versatile and simple eukaryotic model organism. This facultative anaerobe is able to live on various carbon sources, including fermentable and non-fermentable substances. When the yeast is grown on fermentable substrates like glucose, the metabolic energy essentially originates from glycolysis, whereas in the presence of a non-fermentable carbon source, such as glycerol, the mitochondrial oxidative metabolism is fully activated.

ROS cause oxidative modification of cell macromolecules such as proteins, DNA and lipids and induce structure alteration leading, in many cases, to loss of function. A great number of recent reports confirm the Harman “free radical theory of ageing” proposed some fifty years ago although many unknown details still remain. For example, although many proteins are found in an oxidized state during cell senescence [1, 2, 3, 4, 5], the identity of the more relevant targets of oxidation and how their modification can affect cell lifespan remains unknown [6]. In the budding yeast *S. cerevisiae* two types of lifespan can be measured: replicative and chronological. Replicative lifespan is defined as the number of divisions an individual cell

* Corresponding author.

undergoes before dying, whereas chronological lifespan is the length of time a population of yeast cells remains viable, in a non-dividing state, following nutrient deprivation [7]. Chronological ageing is characterized by ROS accumulation and oxidative damage and resembles the ageing process of cells in post-mitotic condition such as neuronal cells [8]. Many authors showed that an increase of ROS intracellular concentration led to a shortening of the life span of yeast cells [9, 10]. For this reason, chronological ageing of yeast cells has been extensively used as a model with which to explore several features of ROS production and oxidative damage [11, 12, 13, 14]. So far caloric restriction has been the only way to increase lifespan in all organisms tested [15]. The beneficial effects of caloric restriction on mitochondrial respiration, reactive oxygen species release, replicative and chronological lifespan has recently been studied [16]. Specific markers of ageing, such as protein oxidation as well as iron accumulation and lipofuscin presence, were also decreased in caloric-restricted cells [17]. Owing to the high reactivity of cysteine residues with ROS, their oxidation can be used to monitor the redox status of the cells during all processes that foresee an increase of ROS concentration. Thiol groups play a wide range of roles in cells, since their redox state can affect the activity and the structure of enzymes, receptors, transcription factors, etc. The cysteine residue exists in fully reduced form (-SH) and in different oxidation states: the thiyl radical (S^{\cdot}), the disulfide bond (Cys-S-S-Cys), the sulfenic (-SOH), sulfinic (SO_2H), sulfonic (- SO_3H) acid forms and the nitrosylated form (-S-NO). The cysteine sulfenic and sulfonic acids are irreversible protein oxidation forms with the exception of the cysteine sulfinic acid of peroxiredoxin that is enzymatically reduced by sulphiredoxin [18]. In most cases cysteine oxidation can alter protein function. Otherwise, partial oxidation (disulfide bond or sulfenic acid form) is reversible and is known to play an important role in the regulation of transcription factors, for example Yap1 in *S. cerevisiae* [19], and several phosphotyrosine phosphatases in mammals [20]. Recently S-nitrosylation was found to take place in *S. cerevisiae* although the mechanism of NO production is still a matter for debate because of the lack of mammalian nitric oxide synthase (NOS) orthologues in the yeast genome [2]. However, Castello et al. found that yeast cells are capable of producing NO in mitochondria under hypoxic conditions [21]. In our study, a proteomic approach that combines selective labelling of proteins containing reduced cysteine residues with two-dimensional electrophoresis and mass spectrometry was used to evaluate the redox state of yeast protein cysteines during chronological

ageing. The procedure was developed on the grounds that biotin-conjugated iodoacetamide (BIAM) specifically reacts with reduced cysteine residues [22, 23]. The yeast cells were grown on different carbon sources: 2% glucose, 0.5% glucose and 3% glycerol respectively. Cell lysates were incubated with BIAM and the labelled proteins were separated by two-dimensional electrophoresis and identified by mass spectrometric procedures. Proteins with oxidized cysteine residues were unable to react with BIAM and could easily be identified. These data were integrated with several results on mitochondria morphology and function, ROS production and glutathione protection. Altogether, these data demonstrated that caloric restriction and glycerol extend *S. cerevisiae* lifespan and that oxidative damage in cells grown on standard glucose content essentially occurs on glycolytic enzymes.

Materials and methods

Strains. The strains used in this study were W303-1A (MATa leu2-3,112ura3-1 trp1-92 his3-11,15 ade2-1 can1,100, GAL SUC mal) and W303 transformed with the plasmid pYX232-mtGFP [24], which allows a constitutive expression of mitochondria-targeted GFP.

Chronological life span. Yeast cells were grown at 30 °C in synthetic complete (SC) medium (0.67% yeast nitrogen base without amino acid) supplemented with complete amino acid dropout solution and a fourfold excess of leucine, tryptophan, adenine, histidine, and uracil. These supplements were added in excess to prevent any growth limitation due to the auxotrophies of W303 strain. For W303 + pYX232-mtGFP tryptophan was excluded in order to have plasmid selection. 2% glucose (SCD), 0.5% glucose (CR) or 3% glycerol plus 0.1% glucose (SCG) were used as carbon sources. For chronological ageing experiments, cells were picked from fresh colonies and grown overnight in SCD, CR, and SCG. Cells were then diluted in their respective fresh media to 10^6 cells/ml using flasks with volume/medium ratio of 3:1. Growth was monitored by measuring the turbidity of the culture at 600 nm (OD_{600}) on a spectrophotometer. To determine the number of viable cells, serial dilutions of chronologically ageing cells were plated on YEPD plates. The percentage of colony-forming units (c.f.u.) of chronologically aged cells was obtained by relating the c.f.u. counts to those at the maximum peak of growth, which was considered to be 100%. Viability was defined as the ability of a single cell to form a colony within two days.

Cysteine residues labelling. Cells grown in SC medium supplemented with 2 % glucose, 0.5 % glucose or 3 % glycerol were harvested in exponential phase (10^7 cells/ml) and after 24, 48, 72 hours and one week. For mono-dimensional electrophoresis, cells were broken in RIPA buffer (50 mM Tris-HCl pH 7, 1 % NP-40, 150 mM NaCl, 2 mM EGTA, 100 mM NaF) plus a cocktail of yeast protease inhibitors (Sigma) containing 40 μ M biotinylated iodoacetamide, BIAM (Molecular Probes) with glass beads in a Fastprep instrument (Savant). Protein extracts were clarified by centrifugation at 8000 g for 10 min. For 2D-GE, cells were broken in 8 M urea, 4 % CHAPS, 40 μ M BIAM, Tris-HCl pH7. In both cases the labelling reaction was stopped with 10 mM DTT.

Electrophoresis and Western blot. For mono-dimensional electrophoresis the labelled samples were applied on SDS-PAGE and transferred on PVDF membrane (Millipore). For 2D-GE, IEF was carried out on non-linear wide-range immobilized pH gradients (pH 3 – 10; 18 cm long IPG strips; GE Healthcare, Uppsala, Sweden) in an EttanTM IPG-phorTM system (GE Healthcare, Uppsala, Sweden). Analytical-run IPG strips were rehydrated with 60 μ g of total proteins in 350 μ l of lysis buffer and 0.5 % (v/v) carrier ampholyte for 1 hour at 0 V and for 8 hours at 30 V, at 16 °C. The strips were then focused according to the following electrical conditions at 16 °C: 200 V for 1 hour, from 300 V to 3500 V in 30 min, 3500 V for 3 hours, from 3500 V to 8000 V in 30 min, 8000 V until a total of 80 000 Vh was reached. For preparative gels a load of 400 μ g of total proteins was used. After focusing, analytical and preparative IPG strips were equilibrated for 12 min in 6 M urea, 30 % (v/v) glycerol, 2 % SDS, 0.05 M Tris-HCl, pH 8.8, 2 % DTE, and subsequently for 5 min in the same urea/SDS/Tris buffer solution but substituting the 2 % DTE with 2.5 % iodoacetamide. The second dimension was carried out on 9 – 16 % polyacrylamide linear gradient gels (18 cm x 20 cm x 1.5 mm) at 40 mA/gel constant current, at 10 °C until the dye front reached the bottom of the gel. Analytical gels were stained with ammoniacal silver nitrate as previously described [25]; MS-preparative gels were stained with colloidal Coomassie [26]. For Western blot of 2-D gels, 150 μ g of total proteins were transferred overnight at 4 °C on PDVF membrane using a constant current of 100 mA. In all cases the blots were incubated for at least four hours with blocking buffer (PBS, 2 % non-fat dry milk, 0.1 % Tween-20). Biotinylated proteins were detected by incubating PVDF membrane with streptavidine conjugated horseradish peroxidase (Biorad). The ECL system (GE Healthcare) was used for signal development. PVDF membranes were stained with Coomas-

sie in order to check the transferring process and to confirm that the load was the same for each sample.

Image analysis. For each condition three gels from independent experiments were used for Coomassie staining and Western blot analysis. Gels and Western blot images were acquired with an Epson expression 1680 PRO scanner. Computer-aided 2D image analysis was carried out using the ImageMaster 2D Platinum 6.0 software (GE Healthcare). In particular, each Western blot image was matched with the image of Coomassie stained gel of the same sample, in order to reveal the correspondence between BIAM signals and spots. Only the reproducible differences of BIAM signals were considered for protein identifications. The apparent isoelectric points and molecular masses of the proteins were calculated with ImageMaster 2D Platinum 6.0 using identified proteins with known parameters as references.

Statistical analysis. Data are average \pm SE of at least three independent experiments or are representative results of similar repetition. The two-tailed non paired Student's t-test was performed using ORIGIN 6.0 (Microcal Software, Inc.).

Protein identification by Mass Spectrometry. TPCK-treated Trypsin, dithiothreitol, and α -cyano-4-hydroxycinnamic acid were from Sigma-Aldrich (St. Louis, MO, USA). All other reagents and solvents were of the highest purity available from Carlo Erba (Milan, Italy).

In situ digestion. Analysis was performed on the Coomassie blue-stained spots excised from the gels. Generally the same spot was picked from two different gels and mass spectral analyses were performed on each spot separately. The excised spots were washed firstly with acetonitrile and then with 0.1 M ammonium bicarbonate. Protein samples were reduced by incubation in 10 mM dithiothreitol (DTT) for 45 min at 56 °C. The cysteines were alkylated by incubation in 5mM iodoacetamide for 15 min at room temperature in the dark. The gel particles were then washed with ammonium bicarbonate and acetonitrile. Enzymatic digestion was carried out with trypsin (12.5 ng/ μ l) in 50 mM ammonium bicarbonate pH 8.5 at 4 °C for 4 hours. The buffer solution was then removed and a new aliquot of the enzyme/buffer solution was added for 18 hours at 37 °C. A minimum reaction volume, enough for the complete rehydration of the gel was used. Peptides were extracted by washing the gel particles with 20 mM ammonium bicarbonate and 0.1 % trifluoroacetic acid in 50 % acetonitrile at room temperature. They were then lyophilised.

MALDI-TOF Mass spectrometry. Positive reflectron MALDI spectra were recorded on a Voyager DE STR instrument (Applied Biosystems, Framingham, MA). The MALDI matrix was prepared by dissolving 10 mg of α -cyano-4-hydroxycinnamic acid in 1 ml of acetonitrile/water (90:10 v/v). Following standard procedures, 1 μ l of matrix was applied to the metallic sample plate and then 1 μ l of analyte was added. Acceleration and reflector voltages were set up as follows: target voltage at 20 kV, first grid at 95 % of target voltage, delayed extraction at 600 ns to obtain the best signal-to-noise ratios and the best possible isotopic resolution with multipoint external calibration using peptide mixture purchased from Applied Biosystems. Each spectrum represents the sum of 1500 laser pulses from randomly chosen spots per sample position. Raw data were analyzed using the computer software provided by the manufacturers and are reported as monoisotopic masses.

nanoLC Mass Spectrometry. A mixture of peptide solution was analysed by LC-MS analysis using a 4000Q-Trap (Applied Biosystems) coupled with an 1100 nano HPLC system (Agilent Technologies). The mixture was loaded on an Agilent reverse-phase pre-column cartridge (Zorbax 300 SB-C18, 5 x 0.3 mm, 5 μ m) at 10 μ l/min (A solvent 0.1 % formic acid, loading time 5 min). Peptides were separated on a Agilent reverse-phase column (Zorbax 300 SB-C18, 150 mm X 75 μ m, 3.5 μ m), at a flow rate of 0.3 μ l/min with a 0 % to 65 % linear gradient in 60 min (A solvent 0.1 % formic acid, 2 % acetonitrile in milliQ water; B solvent 0.1 % formic acid, 2 % milliQ water in acetonitrile). Nano-spray source was used at 2.5 kV with liquid coupling, with a declustering potential of 20 V, using an uncoated silica tip from NewObjectives (O.D. 150 μ m, I.D. 20 μ m, T.D. 10 μ m). Data were acquired in information-dependent acquisition (IDA) mode, in which a full scan mass spectrum was followed by MS/MS of the five most abundant ions (2 s each). In particular, spectra acquisition of MS/MS analysis was based on a survey Enhanced MS Scan. (EMS) from 400 m/z to 1400 m/z at 4000 amu/sec. This scan mode was followed by an Enhanced Resolution experiment (ER) for the five most intense ions. Subsequently MS² spectra (EPI) were acquired using the best collision energy calculated on the bases of m/z values and charge state (rolling collision energy) from 100 m/z to 1400 m/z at 4000 amu/sec. Data were acquired and processed using Analyst software (Applied Biosystems).

MASCOT analysis. Spectral data were analyzed using Analyst software (version 1.4.1) and MS/MS centroid peak lists were generated using the MASCOT.dll script (version 1.6b9). MS/MS centroid peaks were

threshold at 0.1 % of the base peak. MS/MS spectra that have less than 10 peaks were rejected. MS/MS spectra were searched against Swiss Prot database (2006.10.17 version) using the licensed version of Mascot 2.1 (Matrix Science), after having converted the acquired MS/MS spectra in mascot generic file format. The Mascot search parameters were: taxonomy *S. cerevisiae*; allowed number of missed cleavages 2; enzyme trypsin; variable post-translational modifications, methionine oxidation, pyro-glu N-term Q; peptide tolerance 200 ppm and MS/MS tolerance 0.5 Da; peptide charge, from +2 to +3 and top 20 protein entries. Spectra with a MASCOT score < 25 being low quality were rejected. The score used to evaluate the quality of matches for MS/MS data > 30. However, spectral data were manually validated and contained sufficient information to assign peptide sequences.

Confocal microscopy analysis and mitochondria function assay. Cells grown in SD complete medium were harvested at the indicated time. 10⁷ cells were washed twice in 10 mM HEPES buffer, then resuspended in the same buffer and incubated at 30 °C in the dark for 2 hours with dihydrorhodamine 123 (Molecular Probes) in order to demonstrate ROS production. The morphology of mitochondria was visualized in W303 cells using the plasmid pYX232-mtGFP [24] that allows a constitutive expression of mitochondria-targeted GFP. In both cases the cells were washed twice in 10 mM Hepes buffer, immobilized with 0.5 % low melting point agarose and visualized on Leica TCF SP5 confocal microscope.

Cytochrome spectra and respiration. Each cytochrome is characterized by a peak of absorption at a specific wavelength: cytochrome aa₃ = 602 nm (cytochrome c oxidase); cytochrome b = 560 nm; cytochrome c = 550 nm. Differential spectra of reduced and oxidized cells were recorded at room temperature, using a Cary 219 spectrophotometer, following the absorption of cellular samples from 630 nm to 540 nm. The height of each peak relative to the baseline of each spectrum is an index of cytochrome content [27]. Oxygen uptake rate was measured at 30 °C using a Hansatech Oxygraph. 100 μ l of cells in suspension were added in the respiration buffer (0.1M K-Phthalate, pH 5.0). The rate of decrease in oxygen content related to the amount of cells (dry weight) is an index of the respiratory ability of the analyzed strain [28].

Determination of intracellular glutathione level. For reduced and oxidized glutathione assay, 10⁷ cells were harvested, washed twice in water and broken in 250 μ l of ice-cold 1.3 % SSA (1.3 % sulphosalicylic acid/

8mM HCl) with glass beads in a Fastprep instrument (Savant). The lysate was clarified by centrifugation (5 min at 10 000 g) and the total GS amount was evaluated using DTNB colorimetric assay (Cayman). To measure only GSSG, in a separate sample, GSH was derivatized by adding 5 μ l of 2-vinylpyridine to 100 μ l of the sample and shaken for one hour prior to the colorimetric assay. The GSSG/GSH ratio was calculated as a percentage of GSSG level in relation to GSH level. Intracellular values of the GSSG/2GSH half cell redox potential were calculated from the intracellular concentration of GSSG and GSH using the Nernst equation:

$$E_{h=} = E_o + 2,303 (kT/nF) \log([GSSG]/[GSH]^2)$$

where E_o is the standard electrode potential (-240 mV) for reduced glutathione at pH7, k is Boltzmann's constant (8.31 J mol⁻¹ K⁻¹), T is the absolute temperature, n is the number of electrons transferred (2) and F is the Faraday constant (96 406 J V⁻¹) [29].

Results

Caloric restriction and glycerol increase chronological life span. *S. cerevisiae* cells were grown in synthetic complete (SC) medium containing three different carbon sources: 2% glucose, 0.5% glucose and 3% glycerol. SC plus 2% glucose (SCD) corresponds to the standard medium used to study chronological ageing features [7], whereas the reduction from 2% to 0.5% glucose content in the media is a model leading to caloric restriction (CR) in yeast [16]. When the glucose level is limited, yeast cells prefer respiration to fermentation and pyruvate is directed to the mitochondria, thus increasing electrons transport and respiration. The ability of 3% glycerol (SCG) and/or caloric restriction (CR) to extend chronological lifespan of yeast cells was examined. Cell viability on different carbon sources was determined by measuring the percentage of colony-forming units (c.f.u.) of yeast cells during ageing. Figure 1 shows that the viability of yeast strains varies dramatically in different media conditions, as also reported by others [4, 7, 16]. When *S. cerevisiae* was grown in SCD, less than 10% of cells were viable after 10 days, on the contrary more than 50% of the cells were still viable after the same period when the cells were cultured in CR. Moreover, growing on a respiratory substrate such as SCG made more than 40% of the yeast cells viable after 10 days.

According to these results, yeast cells grown for 72 hours were selected as our model for chronologically aged cells in all the experiments, since at this point in time the yeast cells, in late stationary growth phase (non-dividing cells), gradually age but are still alive.

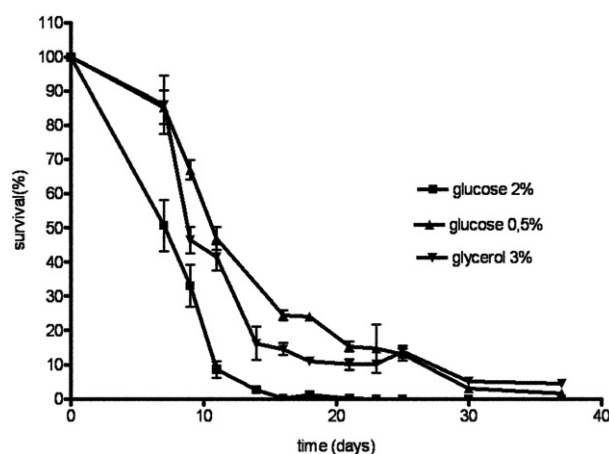


Figure 1. Cell viability on different carbon sources. The percentage of colony-forming units (c.f.u.) of yeast cells was obtained by relating the c.f.u. counts of cells during ageing to those at the beginning of stationary phase which were considered to be 100%. The graphic is representative of three independent experiments.

ROS production and mitochondria morphology during chronological ageing on different carbon sources.

The relationship between ageing and oxidative stress was verified in SCD, SCG and CR by evaluating the amount of ROS production with Dihydrorhodamine 123 (DHR123) [30, 31]. A relatively low and comparable ROS production was observed in yeast cells in the exponential growth phase independent of the different carbon sources (data not shown). When the ROS level was compared in chronologically aged cells (72 hours), oxidation of DHR was shown to be considerably higher in yeast grown on SCD in comparison to CR or SCG. Figure 2 panel A shows that about 70% of the cells were stained with fluorescent DHR after 72 hours of growth in SCD: this indicates a high level of ROS production. On the contrary, the percentage of fluorescent cells after the same period of growth was less than 20% in CR or SCG. Since mitochondria constitute the major source of ROS generation in cells, the morphology of mitochondria in aged cells was analyzed using the plasmid pYX232-mtGFP that allows GFP to be specifically located in these organelles. The mitochondria structure changes depending on the medium; in fact, cells exponentially growing in CR – and even more so in SCG – show several but small mitochondria, whereas in cells growing in a 2% glucose medium they are few, large and branched (described as mitochondria reticula) (Fig. 2B). During ageing in CR and SCG the mitochondria appear progressively more numerous and present a clear spherical shape. Even the mitochondria morphology of SCD grown cells tends to become similar to the one in CR and SCG by passing to the derepressed state characteristic of low glucose level [32], although some cells tend to

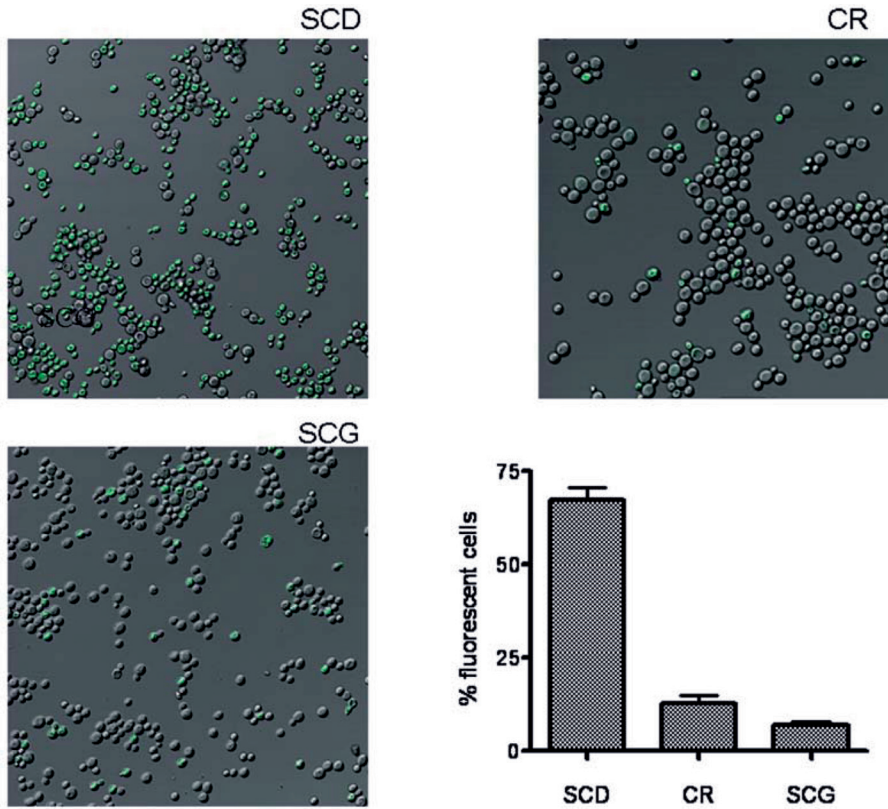
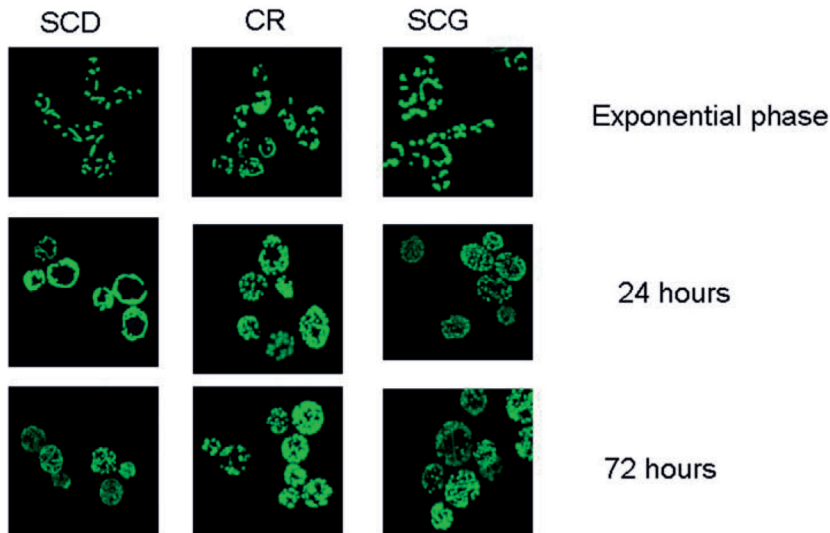


Figure 2. ROS production and GFP mitochondria staining. (A) ROS production, evaluated using the DHR123 fluorescent probe in 72 hours aged cells: figures represent a merge between DIC and fluorescent images obtained with a 40X objective. In the histogram, the percentage of fluorescent cells stained with DHR123 after 72 hours is shown. (B) mitochondria morphology of W303 cells transformed with the plasmid harbouring the mitochondria targeted GFP (pYX232-mtGFP): representative images of mitochondria structure changes during ageing in the different carbon sources. Images were obtained with a confocal microscope using a 63X objective.

A



B

retain mitochondria with filamentous morphology. It is interesting to note that the number of GFP-labelled yeast cells drastically decreased during ageing in SCD compared to the other two conditions (Fig. 2C). This

decrease is already clear after 48 hours (data not shown); this likely indicates that the aged cells in SCD are not proficient in retaining or in correctly reproducing functional mitochondria.

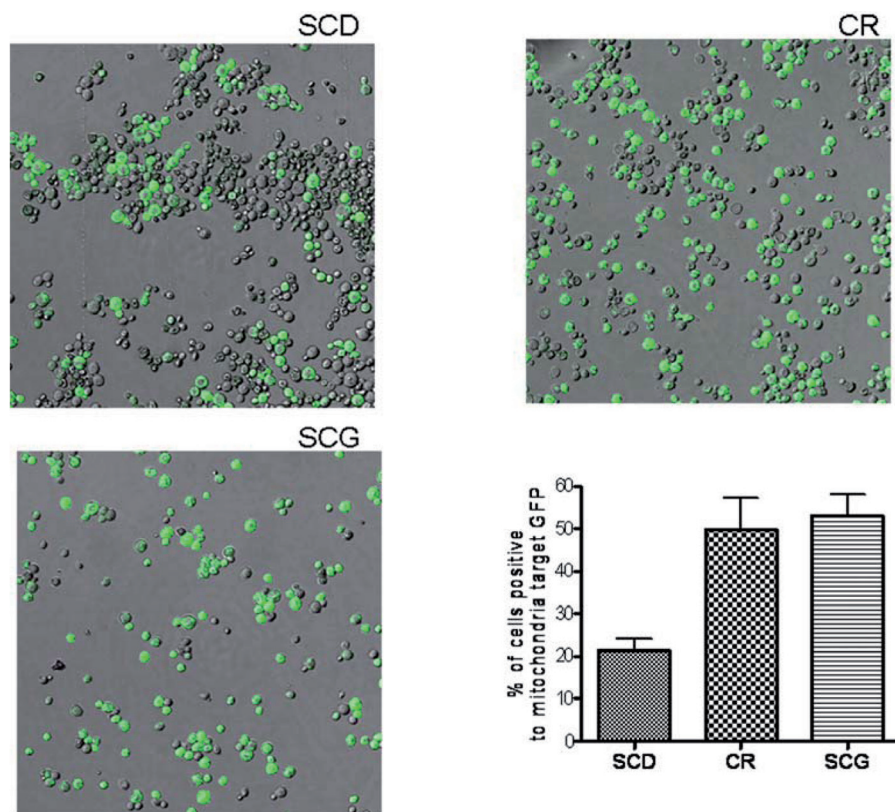


Figure 2. (continued) (C) GFP positive cells: % of cells harbouring visible mitochondria after 72 hours of growth is reported in the histogram and in representative images. Data shown in the histograms represent mean and standard deviation obtained counting four different fields from three independent experiments. The differences of SCG and CR versus SCD are statistically significant as shown by two-tailed non paired Student's t-test (p-value < 0.001 for ROS production experiment and p-value < 0.05 for GFP experiment).

C

O₂ consumption and cytochrome content during chronological life span on different carbon sources.

The respiration ability was measured by evaluating the rate of mitochondrial oxygen consumption. As shown in Figure 3A, after 24 hours similar values of the oxygen consumption rate were observed, independent of growth conditions. However, after 72 hours of growth, the oxygen consumption decreased to 35 % of the consumption rate measured at 24 hours for the cells in SCD, while a lower decrease was observed for those in SCG (70 %) and CR (50 %). The decrease in respiration observed in yeast cells grown in 2% glucose might have been related to an alteration of the amount of the various cytochromes. The mitochondrial cytochrome content was then assessed by spectroscopic analyses. As shown in Figure 3B, after 24 hours cytochromes aa₃, b, and c are present in the yeast grown in all of the analyzed media. However, the amount of cytochrome c was lower in the yeast grown in SCD in comparison to SCG and CR, with this deficiency increasing after 72 hours, as is indicated by the relative heights of the peaks corresponding to cytochromes c, and b.

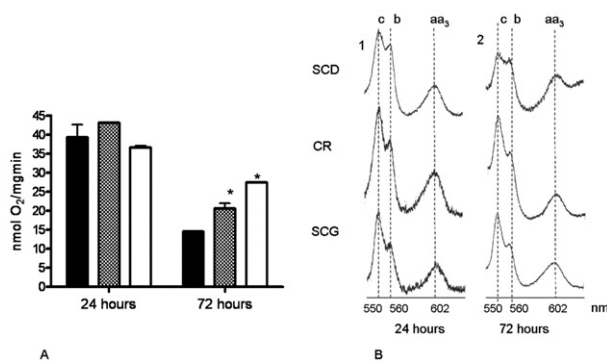


Figure 3. O₂ consumption and cytochromes spectra. A, O₂ consumption was measured using a Hansatech Oxygraph during growth in SCD (black bars), CR (squared bars) and SCG (white bars) growth conditions. After 72 hours of growth O₂ consumption in SCG and CR is significantly higher than in SCD as shown by two-tailed non paired Student's t-test (p-value < 0,05). B, Oxidized versus reduced cytochromes spectra of W303 strain cultured in SDC medium supplemented with the indicated carbon source after 24 hours (1) and 72 hours (2) of growth at 28 °C. The peaks at 550, 560 and 602 nm correspond to cytochromes c, b and aa₃, respectively. The height of each peak relative to the baseline of each spectrum is an index of cytochrome content.

Detection of oxidation-sensitive protein cysteines during chronological ageing on different carbon

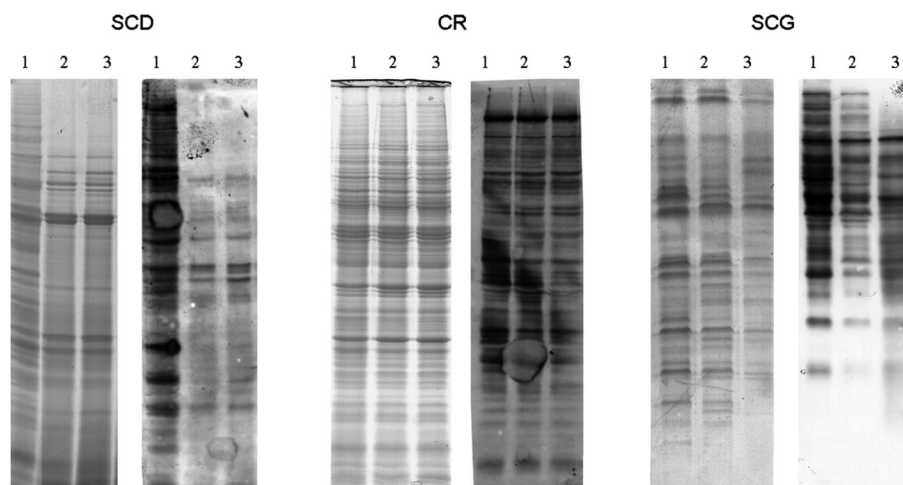


Figure 4. Coomassie staining and blot analysis with HRP-conjugate streptavidin of protein extracts from yeast grown in SCD, CR and SCG. Yeast cells were harvested in exponential phase (lane 1), and after 24 and 72 hours of growth (lane 2 and 3 respectively).

sources. The oxidation of protein cysteines in yeast cells grown in different conditions was investigated by using the BIAM labelling protocol [22]. This procedure leads to a selective biotinylation of proteins that contain reduced cysteine residues. These experiments can easily be monitored by Western blot analyses by taking advantage of the high interaction of biotin with streptavidin. Proteins from yeast cells grown on different carbon sources in exponential phase and during chronological ageing were extracted at pH 7 and incubated with BIAM for 30 min at room temperature. When the BIAM-labelled reaction mixtures were fractionated by mono-dimensional SDS-PAGE followed by Western blot analyses using streptavidin HRP, a clear time-dependent decrease in the amount of BIAM labelled proteins was observed in lysates from SCD cells in comparison to the protein mixtures from cells in CR or in SCG. The results are reported in the Western blot of Figure 4 showing that, in exponential phase, the amount of BIAM-labelled proteins is almost the same in all conditions; in the figure it is evident that after 24 hours the intensity of BIAM signal in SCD cells is drastically reduced and protein degradation is not evident in this condition. Similar mono-dimensional electrophoresis experiments were performed in order to choose better conditions for 2D-GE analysis. In every experiment, each sample was used both for Western blot and for Coomassie staining analysis in order to verify the quality of protein lysates. Moreover, PVDF membranes were stained with Coomassie in order to check the transferring process and to confirm that the load of total proteins was the same for each sample.

In order to identify the major targets of oxidation during chronological ageing in SCD, we selected cells in exponential growth and after 72 hours for the BIAM-labelling protein analysis. Proteins were then separated by 2D-GE and the BIAM-labelled proteins

were revealed by Western blot. Streptavidin immunostained PVDF membranes of protein lysates from yeast cells grown in SCD, both in the exponential phase and during ageing (after 72 hours), were compared using the ImageMaster 2D Platinum 6.0 software. About 50 spots corresponding to BIAM-modified proteins were clearly detected in exponential phase lysates in repeated trials (Fig. 5A). Among these, nine spots could also be detected in the lysates from aged cells, thus indicating that the cysteine residues of the corresponding proteins were still in their reduced form (circled in Fig. 5A and B). Moreover, 10 spots corresponded to proteins that were not visible during ageing when the gels were silver stained; this suggests that these proteins might not be expressed at a detectable level in stationary phase (data not shown). Finally, the image analysis enabled the identification of 31 streptavidin positive spots (indicated by arrows in Fig. 5A), that were present in the exponential phase lysate and then disappeared during ageing (Fig. 5B). These spots very likely corresponded to proteins that underwent oxidation during ageing. The redox statuses of these spots were analysed by BIAM-labelling also in chronologically aged cells grown in CR (Fig. 5C) and in SCG (Fig. 5D). Western blot images were then compared to the corresponding colloidal Coomassie Blue stained preparative 2D-gel and 25 spots (indicated by arrows and numbers in the representative gel showed in Figure 6) were selected for mass spectral identification by the merging of images analyses.

Identification of major proteins oxidized on cysteine residues. Proteins excised from the gel were reduced, alkylated and, *in situ*, digested with trypsin. The resulting peptide mixtures were directly analysed by MALDI/MS according to the peptide mass fingerprinting procedure. Peaks detected in the MALDI

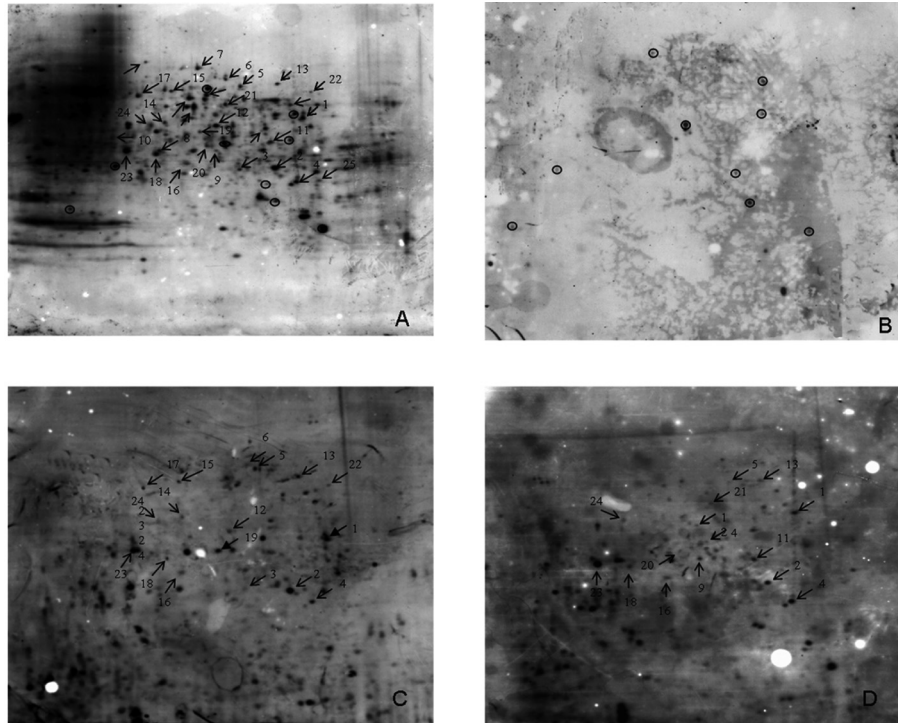


Figure 5. Redox status of cysteine residues during exponential phase and ageing in different carbon sources. Yeast cells were harvested in exponential phase in SCD and after 72 hours of growth in SCD, CR, SCG and treated with 40 μ M BIAM. After 2D-GE, proteins were transferred on PDVF membranes and incubated with streptavidin-HRP in order to detect biotinylated proteins. A, Western blot image of proteins from exponential phase in SCD, arrows and circles indicate, respectively, spots that disappear (arrows) and that are still present (circle) after 72 hours of growth in the same medium. (B), Western blot image of proteins from aged cells in SCD, circles indicate the reactive spots present also in exponential phase. C and D, Western blot images from cells aged in CR and SCG conditions. The spots corresponding to proteins still reduced in aged cells were indicated with arrows and numbers.

spectra were used to search for a non-redundant sequence using the in-house MASCOT software, thus taking advantage of the specificity of trypsin and of the taxonomic category of the samples. The number of measured masses that matched within the given mass accuracy of 200 ppm was recorded and the proteins that had the highest number of peptide matches were examined. The list of proteins identified by this approach is illustrated in Table 1 whilst the sequence coverage of the most relevant proteins obtained by the mass spectral analyses are summarised in Table 1 of supplementary material. Several spots appearing at different molecular mass and isoelectric points were identified as corresponding to the same protein. However, the set of peptides matched by each individual spot clustered in different regions of the corresponding protein sequence, thus suggesting that these multispot protein species originated from proteolytic processing. Thus, together with the intact protein (i.e. spot 1) proteolytically processed forms were identified (spots 2, 3, 4). Moreover, the spectra revealed the presence of some mass signals that could not be assigned to any peptide of the corresponding protein by the MASCOT software. These signals were then manually mapped onto the sequence of the corresponding protein, and this revealed that they had originated from BIAM-modified peptides. For example, Figure 7 shows the partial MALDI spectrum of the tryptic digestion of spot 1, identified as Gapdh. The signals at m/z 2159.1 and 2613.3 were assigned to

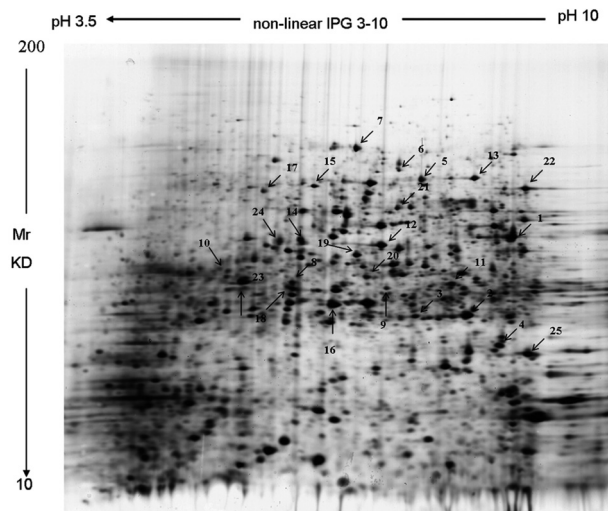


Figure 6. Typical 2D-GE of total proteins from yeast cells grown in 2% glucose. Arrows indicate the spots identified by MS.

the peptide 144–160 that carries one and two BIAM groups, linked to cysteines 150 and 154. Several spots could be not clearly identified by the peptide mass fingerprinting procedure. Additional data were then provided by nanoLC/MS/MS experiments. The peptide mixtures were fractionated by nanoHPLC and sequenced by tandem mass spectrometry. This led to the unambiguous identification of the proteins reported in Table 1. Several major spots (1 to 4) corresponded to glyceraldehyde 3-phosphate dehydrogenase 3 (Gapdh 3), an enzyme involved in

glycolysis and gluconeogenesis. Enolase 1 (Eno1p, Spots 13 and 14) and Enolase 2 (Eno2p, spots 12, 15 and 16) are phosphopyruvate hydratases involved in the conversion of 2-phosphoglycerate to phosphoenolpyruvate during glycolysis and in the reverse reaction during gluconeogenesis. Six spots (from 6 to 11) corresponded to the major isozyme of pyruvate decarboxylase (Pdc1p), whereas spots 22 and 24 were identified as phosphoglycerate kinase (Pgk1p) and fructose-1,6-bisphosphate aldolase (Fba1p), respectively. Finally, spots 17 and 18 resulted in the identification of actin, and spots 20 and 21 were assigned to mannose-1-phosphate guanyltransferase; both proteins are required for normal cell wall structure. In fact, actin is a structural protein involved in many cytoskeletal functions such as cell wall organization and biogenesis [33, 34] whilst mannose-1-phosphate guanyltransferase is an enzyme responsible for cell wall biosynthesis [35].

Effects of growth media and chronological ageing on antioxidant systems. In order to understand whether the antioxidant systems of yeast cells were affected by different growth conditions, the changes in cellular GSH, GSSG concentration, and GSSG/GSH ratio during ageing were monitored by the glutathione reductase-DTNB assay. Figure 8A shows that the GSH and GSSG content was almost identical in all conditions during the exponential phase. However, the GSH concentration drastically decreased during ageing in standard glucose medium in comparison to CR and SCG. Since glutathione represents the main redox system of the cell and offers the greatest contribution to the redox environment, the GSSG/2GSH half cell redox potential (glutathione E_h) was measured. The estimation of the glutathione E_h obtained using the Nernst equation gives a more appropriate measurement of the redox state of the cells compared to the simple oxidized to reduced glutathione ratio. In fact the GSSG/GSH ratio could

be quite a misleading indicator of cell stress; for example, the aged cells (72 hours) grown in SCD and in SCG present the same percentage of GSSG (18%) (Fig. 8A, grey bars), but the E_h in SCG is more negative than in SCD, thus indicating a less oxidative state (Fig. 8B). Our results, demonstrated that a lesser negativity of E_h values in SCD aged cells indicates a condition which is more prone to oxidation.

Discussion

The results reported in this paper demonstrate that the lifespan of *S. cerevisiae* cells was heavily affected by growth in different carbon sources. Although yeast cells, whether grown in SCD, CR or in SCG, did not show major differences in exponential phase, CR and SCG greatly extended the lifespan of chronologically aged cells as compared to SCD. When respiration was the only way to produce ATP, more than 40% of the cells were still viable after 10 days; this might be related to the low production of ROS [36, 37]. In fact an increase in the ROS production could clearly be observed in senescent cells grown in standard glucose concentration. This increase was related to the mitochondria state [38, 39]. During the exponential phase and even more so during ageing, cells grown in CR or SCG displayed small and numerous mitochondria; these differences were previously analysed by Visser [32], who shows that the reticular morphology is associated with a repressed condition typical of growth in high glucose medium or oxygen absence, whereas yeast cells growing on non-fermentable carbon sources display a large number of small mitochondria. This situation is not reproducible in mammalian cells. The mitochondrial morphology of SCD grown cells is reticular in the exponential phase and becomes similar to that observed in CR and in SCG during ageing, although many cells tend to retain mitochondria with filamentous structure. Furthermore a progressive num-

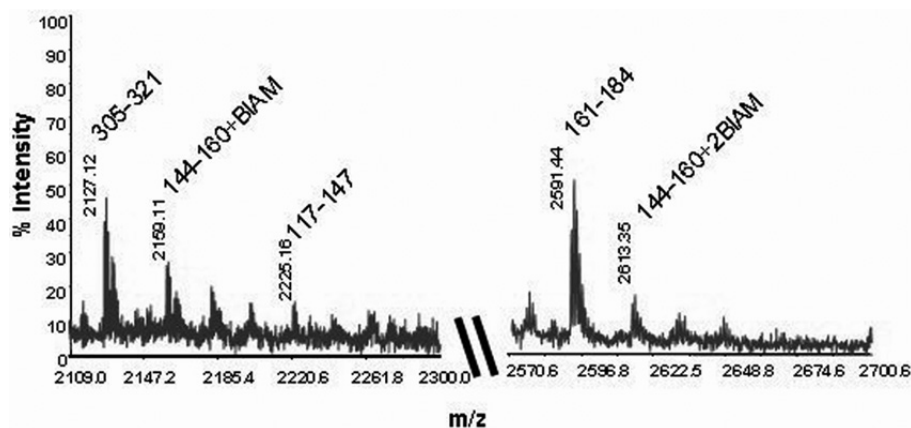


Figure 7. GAPDH is BIAM-labelled in yeast cell exponentially growing. Partial MALDI mass spectrum of the peptide mixture from spot 1. The peptide fragment 144–160 modified with one and two BIAM moieties is reported.

Table 1. Spots' identities of BIAM-labelled proteins in SCD exponential phase

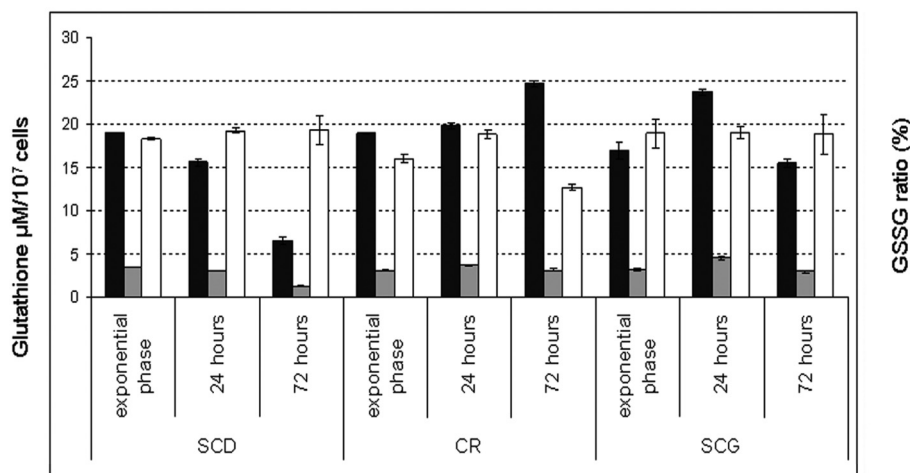
Spot	pI/MW(kDa) theoretical	pI/ MW(kDa) 2DE	Mascot score	No. of peptides	Sequence coverage (%)	Protein	Accession number
1*	6.49/35.71	6.8/32.77	470	33	69	Glyceraldehyde-3-phosphate dehydrogenase 3	P00359
2*	6.49/35.71	6.5/21.01	321	23	46	Glyceraldehyde-3-phosphate dehydrogenase 3	P00359
3*	6.49/35.71	6.25/20.92	127	12	22	Glyceraldehyde-3-phosphate dehydrogenase 3	P00359
4 [#]	6.49/35.81	6.72/19.73	423		VLPELQGK VVDLVEHVAKAK AVGKVLPELQGK TASGNIIPSSTGAAK LNKETYDEIKK GGRTASGNIIPSSTGAAK TASGNIIPSSTGAAKAVGK IVSNASCTTNCLAPLAK	Glyceraldehyde-3-phosphate dehydrogenase 2	P00358
5*	5.98/48.57	6.29/45.53	134	13	30	Protein MET17includes: O-acetylhomoserine sulfhydrylase	P06106
6*	5.8/61.55	6.15/48.86	238	24	46	Pyruvate decarboxylase isozyme 1	P06169
7*	5.8/61.55	6.0/56.62	447	56	56	Pyruvate decarboxylase isozyme 1	P06169
8 [#]	5.8/61.55	5.41/25.65	54		Q-trap	Pyruvate decarboxylase isozyme 1	P06169
9*	5.8/61.55	6.09/25.02	73	17	7	Pyruvate decarboxylase isozyme 1	P06169
10 [#]	5.8/61.55	5.09/27.47	291		LLTTIADAAK NATFPGVQMK TPANAAPASPLK NPVILADACCSR DAKNPVILADACCSR	Pyruvate decarboxylase isozyme 1	P06169
11	5.80/61.55	6.46/25.51	82	8	21	Pyruvate decarboxylase isozyme 1	P06169
12*	5.67/46.81	6.06/31.49	205	17	32	Enolase 2	P00925
13*	6.17/46.70	6.59/45.69	392	42	65	Enolase 1	P00924
14 [#]	5.67/46.81	5.5/32.04	467		TFAEAMR IGSEVYHNLK IGLDCASSEFFK NVPLYQHLADLSK IGSEVYHNLKSLTK AVDDFLLSLDGTANKSK	Enolase 1	P00924
15*	5.67/46.81	5.66/44.04	345	27	47	Enolase 2	P00925
16 [#]	5.67/46.81	5.82/22.87	350		TFAEAMR IGSEVYHNLK IGLDCASSEFFK NVPLYQHLADLSK IGSEVYHNLKSLTK AVDDFLLSLDGTANKSK	Enolase 2	P00925
17*	5.44/41.90	5.24/42.28	138	11	27	Actin	P60010
18 [#]	5.44/41.90	5.34/25.14	206		Q-trap	Actin	P60010
19*	6.26/37.03	6.0/29.83	92	5	27	Alcohol dehydrogenase I	P00331
20*	5.95/39.71	6.01/26.77	111	12	29	Mannose-1-phosphate guanylttransferase	P41940
21*	5.95/39.71	6.15/37.56	143	12	32	Mannose-1-phosphate guanylttransferase	P41940
22*	7.10/44.64	6.88/43.07	423	38	75	Phosphoglycerate kinase	P00560
23*	8.31/23.73	5.15/25.94	434	33	72	Heat shock protein 26	P15992
24*	5.51/39.75	5.03/32.04	180	19	31	Fructose-1,6-bisphosphate aldolase	P14540
25 [#]	9.14/50.40	6.89/19.03	169		IGGIGTVPVGR FQEIWKETSNIK VETGVKPGMVVTFAPAGVTTEVK	Elongation factor 1-alpha	P02994

* Sequence coverage of the protein is reported in Table 1 as material online at Springerlink

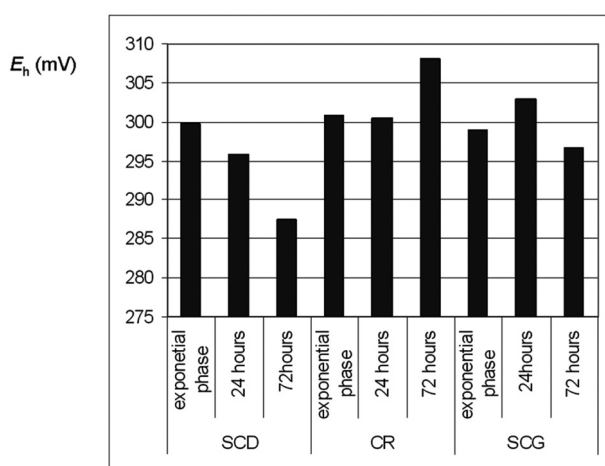
[#] identified by LC/MSMS analysis

ber of cells were observed to lose the mitochondrial GFP signal, this phenomenon being more pronounced for SCD growing cells. A possible explanation is that the damage caused by ROS production affects the mitochondria themselves first and then the entire cell, because the yeast cells grown in standard glucose

medium failed to adapt their mitochondria to an "ageing condition". To further investigate this hypothesis, mitochondrial functions were evaluated by measuring the oxygen consumption of the cells. As expected, senescent cells in SCD clearly showed a decrease of respiration rate probably related to a decrease of



A



B

Figure 8. (continued) (B) Corresponding intracellular half cell redox potential for GSSG/2GSH couple (E_h) was calculated using the Nernst equation, as described in experimental procedures.

cytochrome C amount. The results reported here suggest that growth in standard glucose medium leads to reduced mitochondrial efficiency during chronological ageing, even though during this process the glucose content decreases in the medium to a concentration similar to that in CR [40, 41, 42]. Respiration induced by caloric restriction or by a non-fermentable carbon source seems to induce good mitochondrial metabolic activity with low ROS leakage from the respiratory chain. Many authors reported that a restricted dietary intake increased the rate of oxygen consumption, thus indicating an increase in mitochondrial respiration [43, 44].

Furthermore, an evaluation of the GSH and GSSG levels also suggests that better mitochondrial activity might promote longevity by triggering mechanisms that

Figure 8. Redox state of yeast cells during different growth conditions. (A) intracellular level of GSH (black bars), GSSG (white bars) and GSSG ratio (grey bars) measured with glutathione reductase-DTNB assay during chronological ageing in SCD, CR and SCG conditions. The GSSG/GSH ratio was calculated as a percentage of GSSG level in relation to GSH level.

protect cells against oxidative stress. Growth on CR and SCG promoted an increase of the glutathione content resulting in a more negative E_h value that affects the antioxidant defence of yeast cells. The reduction of the glutathione pool in cells aged in standard glucose medium might be related to an increase in the need of glutathione in the thiol redox system to counteract the increased ROS production. The oxidative effect caused to proteins by ROS generation during ageing was analyzed by evaluating the oxidation state of their cysteine residues. Senescent cells grown in 2% glucose showed a prevalent presence of cysteine residues in their oxidized form. As expected, yeast cells chronologically aged on both reduced glucose and glycerol showed a much lower presence of oxidized cysteine residues. In senescent cells grown on 2% glucose the oxidation targets include actin, mannose-1-phosphate guanyltransferase and enzymes involved in glucose metabolism, most of which belong to the glycolytic pathway (for example: Gapdh, iso-enzyme 3 Pdc1p, Eno1p and Eno2p, Pgk1p and Fba1p). In Table 2 we compare the set of proteins identified in our experiments as having modified SH groups with a set of proteins identified by other authors, using other methods such as detection of protein carbonyls. We tested the Gapdh activity in cell lysates from the three conditions and no significant differences were detected (data not shown). It is known that mammalian Gapdh has different activities, not related to its glycolytic function, including roles in membrane fusion, microtubule bundling, transcription, nuclear RNA transport and regulation of Ca^{2+} homeostasis. In addition Gapdh plays a role in apoptosis, which is probably due to its accumulation in the nucleus [45, 46]. Recent studies have revealed that Gapdh is a redox-sensitive glycolytic enzyme and it is involved in neuronal cell death which is triggered by oxidative stress. In fact this stress induces

Table 2. Protein oxidation targets found in this work in comparison to previous protein identification in *S. cerevisiae*

Protein	Protein modification observed	Condition
Glyceraldehyde-3-phosphate dehydrogenase 3	oxidation: [1, 2] carbonylation: [3, 4], S-thiolation: [5]	oxidative stress, apoptosis, ageing
Protein MET17 includes: O-acetylhomoserine sulfhydrylase	oxidation: [1], this work	oxidative stress
Pyruvate decarboxylase isozyme 1	oxidation: [1], this work carbonylation: [3, 4]	ageing, oxidative stress
Enolase 2	oxidation: [1], this work carbonylation: [3, 4]	ageing, oxidative stress
Enolase 1	oxidation: [1], this work carbonylation: [3, 4]	ageing, oxidative stress
Actin	carbonylation: [4]	ageing
Alcohol dehydrogenase I	carbonylation: [4]	ageing
Mannose-1-phosphate guanyltransferase	oxidation: this work	
Phosphoglycerate kinase	oxidation: [1], this work carbonylation: [3]	oxidative stress
Heat shock protein 26	oxidation: this work	
Fructose-1,6-bisphosphate aldolase	oxidation: [1], this work carbonylation: [3, 4]	ageing, oxidative stress
Elongation factor 1-alpha	oxidation: [1], this work	oxidative stress

amyloid-like aggregation of Gapdh via aberrant disulfide bonds of the active site cysteine. The formation of such abnormal aggregates promotes cell death, thus revealing a new role for this classic glycolytic enzyme [47].

One of the spots identified corresponds to Pdc1p, an enzyme strongly expressed in yeast cells growing on fermentative carbon sources and is thought to have a limited expression in cells grown in respiratory carbon sources. Another of these spots corresponds to alcohol dehydrogenase I (Adh1p), the enzyme responsible for converting acetaldehyde to ethanol during fermentation. During growth in SCG, a respiratory carbon source, Adh1p has a low expression as it is specific for fermentation. Actin was found to be involved in many processes including transcription and remodelling of chromatin structure. Recently it has been demonstrated that cysteines 285 and 374 of actin are important physiological sensors of intracellular oxidative stress and act as regulators of programmed cell death during chronological ageing [48]. On the whole the results obtained on cell viability, mitochondria morphology and functionality and the investigation of the protein oxidation level strongly suggest that the glucose content in the growth medium and its repressive effect on transcription partially determine the fate of yeast cells.

Electronic supplementary material. Supplementary material is available in the online version of this article at springerlink.com (DOI 10.1007/s00018-009-8574-7) and is accessible for authorized users.

Acknowledgements. The plasmid pYX232-mtGFP was kindly provided by Renè Massimiliano Marsano and Tiziana Lodi of Department of Genetics, Anthropology and Evolution, University of Parma, Parma, Italy. The authors would like to express their thanks to Dr. T. Fiaschi for her support with the confocal microscopy and Prof. C. Falcone for critical reading of the manuscript. This work was supported by MIUR-PRIN 2003 and MIUR-PRIN 2005 grants.

- 1 Le Moan, N., Clement, G., Le Maout, S., Tacnet, F., and Toledano, M. B. (2006). The *Saccharomyces cerevisiae* proteome of oxidized protein thiols: contrasted functions for the thioredoxin and glutathione pathways. *J. Biol. Chem.* 281, 10420–30.
- 2 Almeida, B., Buttner, S., Ohlmeier, S., Silva A., Mesquita, A., Sampaio-Marques, B., Osório N. S., Kollau, A., Mayer, B., Leão, C., Laranjinha, J., Rodrigues, F., Madeo, F., and Ludovico, P. (2007). NO-mediated apoptosis in yeast. *J. Cell Sci.* 120, 3279–88.
- 3 Yoo, B. S., and Rainier, F. E. (2004). Proteomic analysis of carbonylated proteins in two-dimensional gel electrophoresis using avidin-fluorescein affinity staining. *Electrophoresis* 25, 1334–41.
- 4 Reverter-Branchat, G., Cabisco, E., Tamarit, J., and Ros, J. (2004). Oxidative damage to specific proteins in replicative and chronological-aged *Saccharomyces cerevisiae*: common targets and prevention by calorie restriction. *J. Biol. Chem.* 279, 31983–9.
- 5 Shenton, D., Perrone, G., Quinn, K. A., Dawes, I. W., and Grant, C. M. (2002). Regulation of protein S-thiolation by glutaredoxin 5 in the yeast *Saccharomyces cerevisiae*. *J. Biol. Chem.* 277, 16853–9.
- 6 Balaban, R. S., Nemoto, S., and Finkel, T. (2005). Mitochondria, oxidants, and ageing. *Cell* 120, 483–95.
- 7 Fabrizio, P., and Longo, V. D., (2003). The chronological life span of *Saccharomyces cerevisiae*. *Ageing Cell.* 2, 73–81.
- 8 Laun, P., Rinnerthaler, M., Bogengruber, E., Heeren, G., and Breitenbach, M. (2006). Yeast as a model for chronological and reproductive ageing: a comparison. *Exp. Gerontol.*, 41, 1208–12.

- 9 Passos, J. F., and Von Zglinicki, T. (2006). Oxygen free radicals in cell senescence: are they signal transducers? *Free Radic. Res.* 40, 1277–83.
- 10 Unlu, E. S., and Koc, A. (2007). Effects of deleting mitochondrial antioxidant genes on life span. *Ann. N. Y. Acad. Sci.* 1100, 505–9.
- 11 Fabrizio, P., Pozza, F., Pletcher, S. D., Gendron, C. M., and Longo, V. D. (2006). Regulation of longevity and stress resistance by Sch9 in yeast. *Science* 292, 288–90.
- 12 Longo, V. D. (2003). The Ras and Sch9 pathways regulate stress resistance and longevity. *Exp. Gerontol.* 38, 807–11.
- 13 Longo, V. D., Gralla, E. B., and Valentine, J. S. (1996). Superoxide dismutase activity is essential for stationary phase survival in *Saccharomyces cerevisiae*. Mitochondrial production of toxic oxygen species in vivo. *J. Biol. Chem.* 271, 12275–80.
- 14 Bonawitz, N. D., Chatenay-Lapointe, M., Pan, Y., and Shadel, G. S. (2007). Reduced TOR signaling extends chronological life span via increased respiration and upregulation of mitochondrial gene expression. *Cell Metab.* 5, 265–77.
- 15 Koubova, J., and Guarente, L. (2003). How does calorie restriction work? *Genes Dev.* 17, 313–21.
- 16 Lin, S. J., Kaerberlein, M., Andalis, A. A., Sturtz, L. A., Defossez, P. A., Culotta, V. C., Fink, G. R., and Guarente, L. (2003). Calorie restriction extends *Saccharomyces cerevisiae* lifespan by increasing respiration. *Nature* 418, 344–8.
- 17 Reverter-Branchat, G., Cabisco, E., Tamarit, J., and Ros, J. (2004). Oxidative damage to specific proteins in replicative and chronological-aged *Saccharomyces cerevisiae*: common targets and prevention by calorie restriction. *J. Biol. Chem.* 279, 31983–9.
- 18 Biteau, B., Labarre, J., and Toledano, M. B. (2003). ATP-dependent reduction of cysteine-sulphinic acid by *S. cerevisiae* sulphiredoxin. *Nature* 425, 980–4.
- 19 Wood, M. J., Storz, G., and Tjandra, N. (2004). Structural basis for redox regulation of Yap1 transcription factor localization. *Nature* 430, 917–21.
- 20 Denu, J. M., and Tanner, K. G. (1998). Specific and reversible inactivation of protein tyrosine phosphatases by hydrogen peroxide: evidence for a sulfenic acid intermediate and implications for redox regulation. *Biochemistry* 37, 5633–42.
- 21 Castello, P. R., David, P. S., McClure, T., Crook, Z., and Poyton, R. O. (2006). Mitochondrial cytochrome oxidase produces nitric oxide under hypoxic conditions: implications for oxygen sensing and hypoxic signaling in eukaryotes. *Cell Metab.* 3, 277–87.
- 22 Kim, J. R., Yoon, H. W., Kwon, K. S., Lee, S. R., and Rhee, S. G. (2000). Identification of proteins containing cysteine residues that are sensitive to oxidation by hydrogen peroxide at neutral pH. *Anal. Biochem.* 283, 214–21.
- 23 Ramachandran, A., Ceaser, E., and Darley-Usmar, V. M. (2004). Chronic exposure to nitric oxide alters the free iron pool in endothelial cells: role of mitochondrial respiratory complexes and heat shock proteins. *Proc. Natl. Acad. Sci.* 101, 384–9.
- 24 Westermann, B., and Neupert, W. (2000). Mitochondria-targeted green fluorescent proteins: convenient tools for the study of organelle biogenesis in *Saccharomyces cerevisiae*. *Yeast* 16, 1421–7.
- 25 Hochstrasser, D. F., Patchornik, A., and Merrill, C. R. (1998). Development of polyacrylamide gels that improve the separation of proteins and their detection by silver staining. *Anal. Biochem.* 173, 412–23.
- 26 Vilain, S., Cosette, P., Charlionet, R., Hubert, M., Lange, C., Junter, G. A., and Jouenne, T. (2001). Substituting Coomassie brilliant blue for bromophenol blue in two dimensional electrophoresis buffers improves the resolution of focusing patterns. *Electrophoresis* 22, 4368–4374.
- 27 Dequard, M., Couderc, J. L., Legrain, P., Belcour, L., and Picard-Bennoun, M. (1980). Search for ribosomal mutants in *Podospora anserina*: genetic analysis of mutants resistant to paromomycin. *Biochem. Genet.* 18, 263–280.
- 28 Foury, F. (1989). Cloning and sequencing of the nuclear gene MIP1 encoding the catalytic subunit of the yeast mitochondrial DNA polymerase. *J. Biol. Chem.* 264, 20552–20560.
- 29 Hwang, C., Lodish, H. F., and Sinskey, A. J. (1995). Measurement of glutathione redox state in cytosol and secretory pathway of cultured cells. *Methods Enzymol.* 251, 212–21.
- 30 Unterluggauer, H., Hampel, B., Zwerschke, W., and Jansen-Dürr, P. (2003). Senescence-associated cell death of human endothelial cells: the role of oxidative stress. *Exp Gerontol.* 38, 1149–60.
- 31 Madeo, F., Frohlich, E., Ligr, M., Grey, M., Sigrist, S. J., Wolf, D. H., and Frohlich, K. U. (1999). Oxygen stress: a regulator of apoptosis in yeast. *J. Cell. Biol.* 145, 757–67.
- 32 Visser, W., van Spronsen, E. A., Nanninga, N., Pronk, J. T., Gijs Kuenen, J., and van Dijken, J. P. (1995). Effects of growth conditions on mitochondrial morphology in *Saccharomyces cerevisiae*. *Antonie Van Leeuwenhoek.* 67, 243–53.
- 33 Moseley, J. B., and Goode, B. L. (2006). The yeast actin cytoskeleton: from cellular function to biochemical mechanism. *Microbiol. Mol. Biol. Rev.* 70, 605–45.
- 34 Gourlay, C. W., and Ayscough, K. R. (2005). The actin cytoskeleton: a key regulator of apoptosis and ageing? *Nat. Rev. Mol. Cell. Biol.* 6, 583–9.
- 35 Yoda, K., Kawada, T., Kaibara, C., Fujie, A., Abe, M., Hashimoto, H., Shimizu, J., Tomishige, N., Noda, Y., and Yamasaki, M. (2000). Defect in cell wall integrity of the yeast *Saccharomyces cerevisiae* caused by a mutation of the GDP-mannose pyrophosphorylase gene VIG9. *Biosci. Biotechnol. Biochem.* 64, 1937–1941.
- 36 Drakulic, T., Temple, M. D., Guido, R., Jarolim, S., Breitenbach, M., Attfield, P. V., and Dawes, I. W. (2005). Involvement of oxidative stress response genes in redox homeostasis, the level of reactive oxygen species, and in *Saccharomyces cerevisiae*. *FEMS Yeast Res.* 5, 1215–28.
- 37 Bonawitz, N. D., Rodeheffer, M. S., Shadel, G. S. (2006). Defective mitochondrial gene expression results in reactive oxygen species-mediated inhibition of respiration and reduction of yeast life span. *Mol. Cell. Biol.* 26, 4818–29.
- 38 Barros, M. H., Bandy, B., Tahara, E. B., A. J. Kowaltowski. (2004). Higher respiratory activity decreases mitochondrial reactive oxygen release and increases life span in *Saccharomyces cerevisiae*. *J. Biol. Chem.* 279, 49883–49888.
- 39 Stöckl, P., Zankl, C., Hütter, E., Unterluggauer, H., Laun, P., Heeren, G., Bogengruber, E., Herndler-Brandstetter, D., Breitenbach, M., and Jansen-Dürr, P. (2007). Partial uncoupling of oxidative phosphorylation induces premature senescence in human fibroblasts and yeast mother cells. *Free Radic. Biol. Med.* 43, 947–58.
- 40 Osiewacz, H. D., and Scheckhuber, C. Q. (2006). Impact of ROS on two fungal model systems: *Saccharomyces cerevisiae* and *Podospora anserina*. *Free Radic. Res.* 40, 1350–8.
- 41 Kitagaki, H., Araki, Y., Funato, K., and Shimo, H. (2007). Ethanol-induced death in yeast exhibits features of apoptosis mediated by mitochondrial fission pathway. *FEBS Lett.* 581, 2935–42.
- 42 Du, L., Yu, Y., Chen, J., Liu, Y., Xia, Y., Chen, Q., and Liu, X. (2007). Arsenic induces caspase- and mitochondria-mediated apoptosis in *Saccharomyces cerevisiae*. *FEMS Yeast Res.* 7, 860–5.
- 43 Lin, S. J., Kaerberlein, M., Andalis, A. A., Sturtz, L. A., Defossez, P. A., Culotta, V. C., Fink, G. R., and Guarente, L. (2002). Calorie restriction extends *Saccharomyces cerevisiae* lifespan by increasing respiration. *Nature* 418, 344–8.
- 44 Smith, D. L. Jr, McClure, J. M., Matecic, M., Smith, J. S. (2007). Calorie restriction extends the chronological lifespan of *Saccharomyces cerevisiae* independently of the Sirtuins. *Aging Cell* 6, 649–62.
- 45 Magherini, F., Tani, C., Gamberi, T., Caselli, A., Bianchi, L., Bini, L., and Modesti, A. (2007). Protein expression profiles in *Saccharomyces cerevisiae* during apoptosis induced by H₂O₂. *Proteomics* 7, 1434–45.

- 46 Saunders, P. A., Chen, R. W., and Chuang D. M. (1999). Nuclear translocation of glyceraldehyde-3-phosphate dehydrogenase isoforms during neuronal apoptosis. *J. Neurochem.* 72, 925–32
- 47 Nakajima, H., Amano, W., Fujita, A., Fukuhara, A., Azuma, Y. T., Hata, F., Inui, T., and Takeuchi, T. (2007). The active site cysteine of the proapoptotic protein glyceraldehyde-3-phosphate dehydrogenase is essential in oxidative stress-induced aggregation and cell death. *J. Biol. Chem.* 282, 26562–74.
- 48 Farah, M. E., and Amberg, D. C. (2007). Conserved actin cysteine residues are oxidative stress sensors that can regulate cell death in yeast. *Mol. Biol. Cell.* 18, 1359–65.

To access this journal online:
<http://www.birkhauser.ch/CMLS>
